Electric Vehicle Enhanced Fast Charging Enabled by Battery Thermal Management and Model Predictive Control

Qiuhao Hu [*], Mohammad Reza Amini [*], Ashley Wiese [**],
Julia Buckland Seeds [**], Ilya Kolmanovsky [***], Jing Sun [*]

[*] *Department of Naval Architecture and Marine Engineering, University of Michigan, Ann Arbor, MI 48109, USA* (e-mails: {qhhu,mamini,jingsun}@umich.edu)
[**] *Ford Motor Company, Dearborn, MI 48126, USA* (e-mails: {awiese,jbucklan}@ford.com)
[***] *Department of Aerospace Engineering, University of Michigan, Ann Arbor, MI 48109, USA* (e-mail: ilya@umich.edu)

Abstract:
This paper explores the synergy between battery thermal management (BTM) in an electric vehicle (EV) and battery charging. A model predictive control (MPC) based approach is proposed to minimize the energy used for BTM during the drive and fast charging stages and the estimated charging time while enforcing constraints imposed on state-of-charge (SOC), power, and thermal conditions of the battery. An adaptive strategy is developed to adjust the weight of the two competing objectives in the MPC cost function to manage the trade-off between BTM energy consumption and charging time. The sensitivity of the proposed MPC-based BTM strategy to uncertainties in the fast charging station availability is also investigated. Our results show that a 12.3% of decrease in the charging time could be achieved by optimally performing BTM at the cost of negligibly higher BTM energy usage in the case study conducted.

Keywords: Model predictive control, Electric vehicles, Battery fast charging, Integrated power and thermal management

1. INTRODUCTION

Electric vehicles (EVs) are becoming more popular due to their expected advantages in reducing carbon emission, when paired with renewable electricity production (Notter et al., 2010; Choi et al., 2018). However, anxiety about driving range and relatively long charging times impede EV's market penetration (Lee and Park, 2013; Chen et al., 2021). To address these issues, fast-charging stations have been rapidly built in recent years to expand the charging infrastructure (Shafiei and Ghasemi-Marzbali, 2022). While fast-charging technology significantly reduces the charging time, the large charging power, typically higher than 50 kW (Parchomiuk et al., 2019), could result in raising battery temperature over desired thresholds (Keyser et al., 2017; Tomaszewska et al., 2019). Thus, an effective power and thermal management strategy during the fast-charging process is of essential importance for EVs.

Although various approaches have been developed for battery thermal management (BTM) (Masoudi et al., 2015; Amini et al., 2020; Park and Ahn, 2021) and battery charging optimization (Hoke et al., 2014), only a few aim to improve the battery fast charging performance by exploiting the coupling of battery charging power and thermal behavior. In (Hamednia et al., 2022), an optimal BTM was developed to reduce the charging time in cold ambient. The simulation results illustrated that for a cold battery, performing thermal pre-conditioning for the battery prior to charging increases the charging power, and thus reduces the charging time. Moreover, the optimization results presented in (Hamednia et al., 2022) reveal a trade-off among traveling time, energy efficiency, and charging cost. In (Dahmane et al., 2021), an optimal scheduling strategy was proposed for charging an EV to minimize the charging cost and charging time, by

leveraging vehicle to grid connectivity. The charging power degradation caused by low ambient temperature was also considered in (Dahmane et al., 2021) to avoid a lower final state-of-charge (SOC).

Unlike cold ambient conditions, which restrict the battery charging power and thus extend the charging time, hot ambient conditions reduce the heat rejection capacity of the battery and its cooling system. If the heat generation due to fast charging exceeds this reduced cooling capacity, it can lead to throttling of the charging rate to keep the battery within acceptable temperature limits, slowing charging, forcing trade-offs between charging time and/or target battery SOC.

This study proposes a multi-objective model predictive control (MPC) to leverage vehicle usage preview information to precondition battery temperature prior to charging, optimally balancing charging time, target SOC, and thermal management energy consumption. This approach may be particularly beneficial for commercial EVs, where charging time and target SOC requirements are typically determined by the trip/mission after leaving the charging station, and it is also more likely that the vehicle mission is known a priori. For example, a commercial delivery EV may be time constrained by arrival/departure times at designated locations, constraining charging time, while the target SOC may be prescribed by the energy required to complete the scheduled delivery tasks up to the next charging event."

The contributions of this study are threefold. Firstly, an MPC-based integrated power and thermal management (iPTM) strategy is developed for battery fast charging optimization. Secondly, an adaptive strategy is proposed to adjust the weight on the charging time in the MPC

cost function to enforce the soft constraint on the charging time and minimize the BTM energy consumption. Thirdly, the robustness of the algorithm is evaluated against uncertainties in the availability of the fast charging station that impacts the queuing time before the start of charging.

The paper is organized as follows. The power and thermal models representative of a commercial EV are presented in Section 2. Section 3 presents the details of the proposed MPC-based iPTM strategy. The simulation results of the proposed method are presented in Section 4. Finally, Section 5 concludes the paper and outlines possible future directions.

2. POWER AND THERMAL MODELS OF A COMMERCIAL ELECTRIC VEHICLE

The models of the thermal and power subsystems, representative of a commercial EV used in this study are described in this section.

2.1 Battery Power-Balance Model

The equivalent circuit model (He et al., 2011) used to represent the battery SOC dynamics is given as:

$$\dot{SOC} = f_{SOC}(t) = \frac{-I_{bat}}{C_{bat}} = -\frac{U_{oc} - \sqrt{U_{oc}^2 - 4R_{int}P_{bat}}}{2R_{int}C_{bat}}, \tag{1}$$

where I_{bat} and C_{bat} are the battery current and capacity, respectively. Moreover, I_{bat} is determined by the battery power (P_{bat}), open circuit voltage (U_{oc}), and internal resistance (R_{int}). When the vehicle is moving, the battery power is the sum of the vehicle traction power (P_{trac}) and the power consumed for the auxiliary subsystems (P_{aux}):

$$P_{bat} = P_{trac} + P_{aux}. \tag{2}$$

Note that P_{trac} is negative when braking, as the electrical braking system recuperates kinetic energy to charge the battery. When the vehicle is charging at the station, P_{bat} is the auxiliary power minus battery charging power (P_{chg}):

$$P_{bat} = P_{aux} - P_{chg}. \tag{3}$$

In this study, the BTM system is the only auxiliary power demand, which is expressed as:

$$P_{aux} = P_{cl} = \frac{\dot{Q}_{cl}}{COP}, \tag{4}$$

where $\dot{Q}_{cl}$ is the rate of the heat rejection from the battery through the cooling system, and COP is the coefficient of the performance, which describes the efficiency of the cooling system. According to (Lee et al., 2012), COP monotonically decreases with $\dot{Q}_{cl}$, indicating that the efficiency of the cooling system decreases as cooling power demand increases.

2.2 Battery Thermal Model

The battery is modeled as a lumped thermal mass and its temperature dynamics are expressed using the following equation:

$$\dot{T}_{bat} = f_{bat}(t) = \frac{1}{m_{bat,thm}C_{bat,thm}}(\dot{Q}_{gen} - \dot{Q}_{amb} - \dot{Q}_{cl}), \tag{5}$$

where $m_{bat,thm}$, $C_{bat,thm}$ are the battery thermal mass and specific heat capacity, respectively. $\dot{Q}_{gen}$ is the irreversible battery heat generation rate attributed to the internal

resistance and is expressed as $\dot{Q}_{gen} = I_{bat}^2 R_{int}$. $\dot{Q}_{amb}$ is the rate of the heat dissipation to ambient through air convection, which is driven by the temperature difference between ambient and battery.

3. MPC-BASED INTEGRATED POWER AND THERMAL MANAGEMENT OF AN EV

We consider a commercial EV operating under a hot ambient temperature and with a low initial SOC, requiring the battery to be charged at a nearby fast charging station. The objectives of the iPTM for the EV in this study are threefold. Firstly, to ensure the final SOC after charging is above a certain threshold. Secondly, to keep the total charging time within the desired range. Lastly, to minimize the energy consumption for the battery thermal management system while enforcing power and thermal constraints. In a real-world application, the requirements on the final SOC and charging time are typically determined by the type of trip and mission of the commercial vehicle after the charging event.
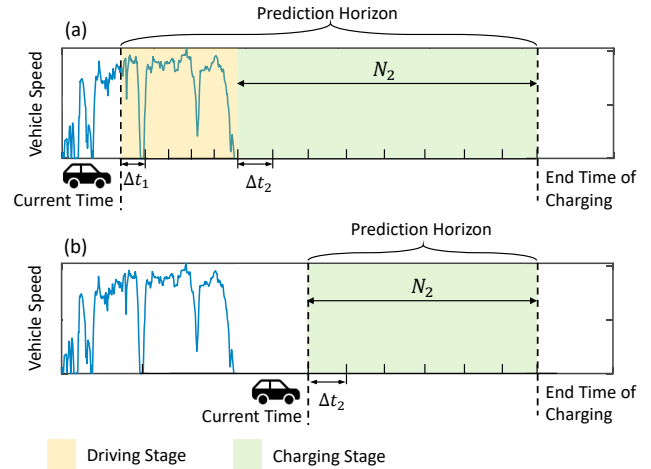

Fig. 1. The implementation concept of the proposed MPC-based iPTM strategy with two different scenarios: (a) before the charging starts, when the vehicle moves towards the charging station, and (b) after the charging starts, when the vehicle stays in the charging station.

To address the aforementioned objectives, an MPC-based iPTM is proposed in this paper. As shown in Fig. 1, two different scenarios, before and after the start of the charging event, are represented. Before the start of the charging event, the vehicle moves towards the charging station, and the prediction horizon of the MPC extends from the current time until the projected end time of the charging event. This time horizon is divided into two stages of driving and charging. After the charging starts, the vehicle stays at the charging station, and the prediction horizon only has one stage from the current time to the end of the charging event. In both cases, the discrete-time finite horizon optimization problem in MPC can be expressed as:

$$\min_{\substack{\dot{Q}_{cl}(i),\\ P_{chg}(i),\, \Delta t_2(i)}} \quad \sum_{i=t}^{t+N_1-1} (\frac{\dot{Q}_{cl}(i)}{COP(i)}\Delta t_1)^2 \; +$$

$$\sum_{i=t+N_1}^{t+N_1+N_2-1} \{(\frac{\dot{Q}_{cl}(i)}{COP(i)}\Delta t_2)^2 + \alpha(\Delta t_2(i))^2 + \beta \epsilon^2\},$$

s.t.
$$SOC(i+1) = SOC(i) + f_{soc}(i)\Delta t_j, \quad j \in \{1,2\}$$
$$T_{bat}(i+1) = T_{bat}(i) + f_{bat}(i)\Delta t_j, \quad j \in \{1,2\}$$
$$SOC(t+N_1+N_2) = SOC_{targ},$$
$$SOC_{min} \le SOC(i) \le SOC_{max},$$
$$T_{bat,min} \le T_{bat}(i) \le T_{bat,max} + \epsilon,$$
$$-\dot{Q}_{cl,max} \le \dot{Q}_{cl}(i) \le 0,$$
$$0 \le P_{chg}(i) \le P_{chg,max},$$
$$0 \le \Delta t_2(i) \le \Delta t_{2,max}, \tag{6}$$

where f_{SOC} and f_{bat} designate the right hand sides of (1) and (5). Δt_1 and Δt_2 are the sampling periods over the driving and charging stages, respectively, and N_1 and N_2 correspond to the numbers of sampling points over these two stages. Therefore, the prediction horizon length is $\Delta t_1 N_1 + \Delta t_2 N_2$ where $\Delta t_1 N_1$ is the remaining time for the vehicle to arrive at the charging station while $\Delta t_2 N_2$ is the total predicted time spent at the charging station. Note that $N_1 = 0$ once the driving is completed and charging started. The index $j \in \{1,2\}$ is determined as follows:

$$j = \begin{cases} 1, & \text{if } i \le t+N_1-1, \\ 2, & \text{if } i \ge t+N_1. \end{cases} \tag{7}$$

It can be seen from (6) that the control/decision variables are $\dot{Q}_{cl}$, P_{chg}, and Δt_2, and the cost function consists of four terms. The first and second terms are the accumulated energy consumption of the battery cooling system over the driving and charging stages. The third term is the square of Δt_2, which penalizes the total charging time. The last term is used to relax the constraint on the battery temperature by introducing a slack variable (ϵ) treating the battery temperature limit as a soft constraint. It avoids infeasibility in solving the discrete-time optimization problem.

As the prediction horizon always extends from the current time to the end of the charging event, the horizon length of the driving stage shrinks over time while the length of the charging stage is not pre-determined and it depends on the computed solution of problem (6) with Δt_2 being an optimization variable. This makes the problem formulation of (6) distinctively different from the conventional receding or shrinking horizon MPC (Amini et al., 2020). To this end, a novel sampling strategy with varying sampling time and sampling points over different optimization horizons is proposed to accommodate the iPTM problem in this study, as summarized here.

During the driving stage, the sampling time Δt_1 is fixed, and N_1 is calculated based on the remaining time before the vehicle arrives at the charging station. However, at the charging stage, the sampling time Δt_2 is one of the adjustable variables determined by the solution of the optimization problem (6), and it is no longer fixed. Instead, the number of samples, N_2, is fixed. Such a sampling strategy allows us to fix the dimension of the optimization problem (6) and solve it numerically. Then, by applying the first element of the computed control sequence to the plant and repeating the optimization with updated initial conditions, a feedback law is formed as in conventional receding horizon MPC scheme.

4. SIMULATION RESULTS AND DISCUSSION

In this section, we present the simulation results of the multi-objective MPC on a commercial EV. A sensitivity analysis is conducted to evaluate the performance of the controller. The ambient temperature is set to be 38^oC and the initial battery SOC is 0.3 (30%). The vehicle goes through an urban route to arrive at the fast charging station, and the battery is required to be charged to $SOC = 0.6$. The maximum battery cooling power and charging power of the station are $5\ kW$ and $80\ kW$, respectively. Moreover, Δt_1 and N_2 are set to 10 sec and 40, respectively.

For this study, during both driving and charging stages, we design the MPC to maintain the battery within an operating range of $15-35\ ^oC$ (Pesaran, 2013; Kim et al., 2019). To discourage violation of the soft temperature constraint, we set the slack variable $\beta = 10^8$, which is large enough to avoid constraint violation over our example use cases.

4.1 Trade-off between BTM energy use and charging time

We first assume that the vehicle speed profile over the urban route is known a priori, based on which the arrival time at the charging station can also be accurately predicted. This assumption will be relaxed in Section 4.3. To investigate the impact of the weight (α) on the charging time in (6), a sensitivity analysis is conducted, and the results are summarized in Fig. 2.
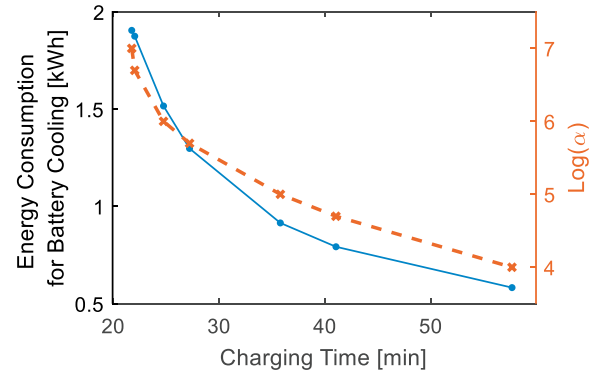

Fig. 2. The energy consumption for battery cooling and battery charging time results with different α.

A trade-off can be observed from Fig. 2 between the energy consumed for battery cooling and battery charging time. As α increases, the battery charging time decreases while the energy consumed for battery cooling increases. To account for the impact of different weights, the state and input trajectories of two cases with different α are presented in Fig. 3. It can be seen that for both cases, thanks to the soft constraint settings and battery cooling system, the battery temperature is maintained within the desired range during the whole process. By comparing the two cases, it can be seen that, with a larger α, the controller tends to draw a larger battery charging power during the charging stage to reduce the charging time, as more focus is put on the penalty term for the charging time in the cost function. However, a larger battery charging power, on the other hand, requires a larger battery cooling power to avoid raising temperature over desired thresholds. Moreover, with accurate knowledge of the arrival time and charging event timing, battery pre-cooling of battery is effected to create some room for the rise of battery temperature, thereby enabling faster charging with larger
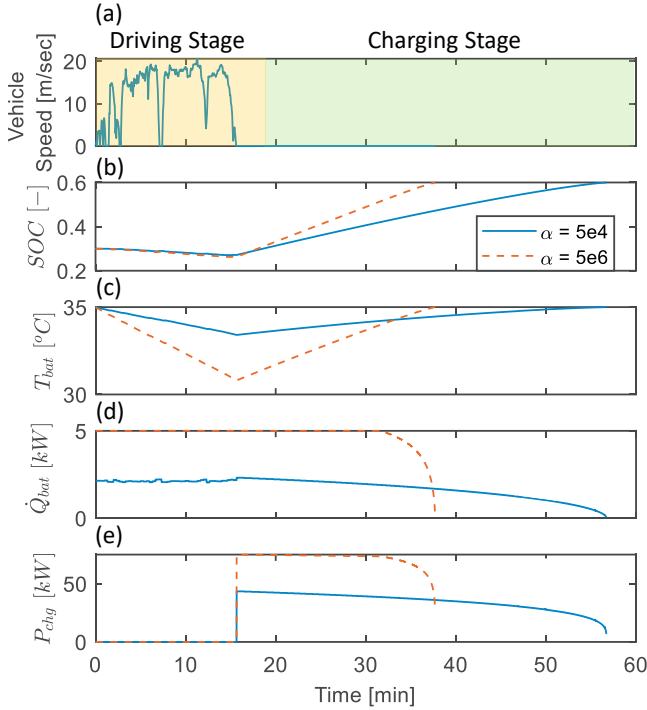
Fig. 3. State and input trajectories with different α values: (a) vehicle speed, (b) SOC, (c) battery temperature, (d) battery cooling power, and (d) battery charging power.

charging power. The above observations explain the trade-off between energy consumed for battery cooling and total charging time, as well as the pre-cooling feature associated with larger α.

4.2 A strategy for weight adaptation

The results shown in Section 4.1 demonstrate that in order to balance the charging time and BTM energy consumption, α needs to be properly tuned to enforce the constraint on charging time while minimizing the energy consumption. There are several challenges of scheduling α in real time. Note that α is determined by the arrival time at the charging station and by the required charging time. It needs to be adjusted during the trip to deal with uncertainties in vehicle speed preview, availability of charging, etc. In this section, an adaptive strategy to schedule α in real-time is proposed, which can be summarized as follows:

- **Step 1**: An initial value of α is selected from the range shown in Fig. 2, at $t = 0$ sec.
- **Step 2**: The optimization problem (6) is solved using the current α_t at time t, and an estimated charging time ($t_{chg,est}$) is calculated as $\Delta t_2 N_2$.
- **Step 3**: α is updated by the following adaptive law:

$$log(\alpha_{t+\Delta t_j}) = log(\alpha_t) + \lambda(t_{chg,est} - t_{chg,req}). \quad (8)$$

- **Step 4**: Repeat Step 2 and 3 till the end of the charging stage.

Here, λ is the adaptation rate, and Δt_j is the sampling time defined in (6). It can been seen that the adaptive law in Step 3 leverages the relationship presented in Fig. 2, and α is updated by comparing the estimated charging time ($t_{chg,est}$) with the required charging time ($t_{chg,req}$). The use of logarithm in the adaptation law (8) allows us to take large step in adaptation over a short period. Given

the range of the α values shown in Fig. 2, conventional linear adaptation will not be able to serve the purpose.

To show the effectiveness of the proposed adaptive strategy for updating α, the required charging time is set to be within 30 min, and different λ values are applied in (8). The simulation results are presented in Fig. 4, and the actual charging times of three cases are summarized in Table. 1. It can be seen that for these three cases, the initial guess for α is too small, which leads to an estimated battery charging time of almost 50 min. With the α updated by the adaptive law, the estimated charging time converges to the value near $t_{chg,req}$. Moreover, as λ increases, the convergence rate increases, and the steady-state error in the final charging time decreases. Based on these results, $\lambda = 0.1$ is adopted for this study, to better adhere to the charging time constraint.
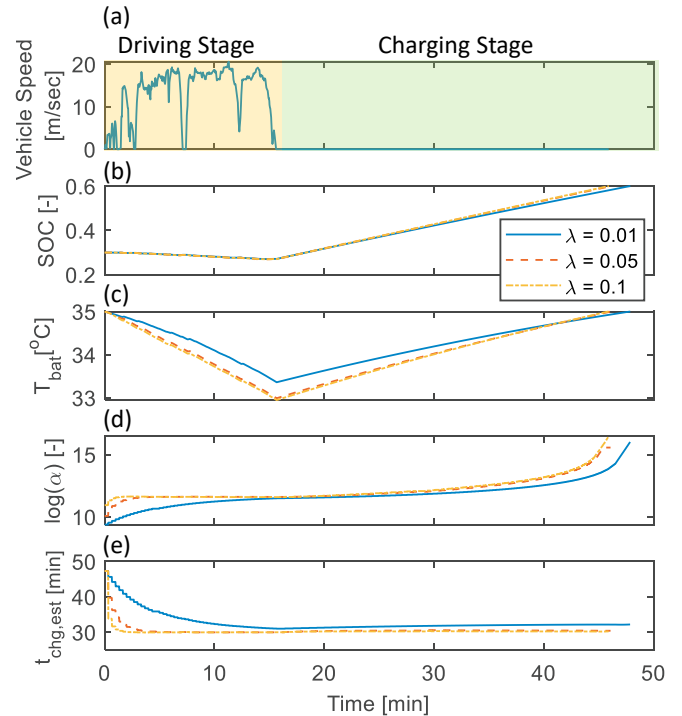

Fig. 4. State and input trajectories with different adaptive rate λ: (a) vehicle speed, (b) SOC, (c) battery temperature, (d) weight on charging time, and (e) estimated charging time.

Table 1. The actual charging time with different adaptive rates.

λ	0.01	0.05	0.1
t_{chg} [min]	32.2	30.4	30.2
BTM energy consumption [kWh]	1.00	1.06	1.07

It can be seen in Figs. 3 and 4 that, MPC incorporates the knowledge of the upcoming charging event to pre-cool the battery, allowing larger battery charging power to reduce the charging time. To quantify the benefits of leveraging the preview information and identify the conditions under which the pre-cooling is beneficial, the following three cases are considered for comparison:

- **Case I**: The charging event is predicted accurately over the prediction horizon,
- **Case II**: The charging event is not predicted until the vehicle arrives at the charging station, and the maximum cooling power is 5 kW,
- **Case III**: The charging event is not predicted until the vehicle arrives at the charging station, and the maximum cooling power is 3 kW.
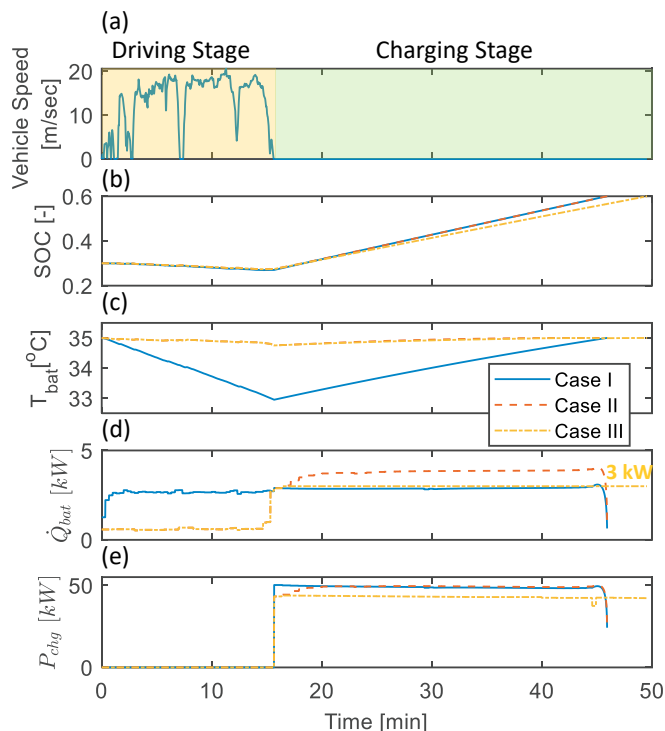
Fig. 5. State and input trajectories with different α for Cases I, II, and III: (a) vehicle speed, (b) SOC, (c) battery temperature, (d) battery cooling power, and (d) battery charging power.

For Case I, it is assumed that the preview information is known a priori, and the proposed MPC-based iPTM is applied at driving and charging stages. For Case II and Case III, before vehicle arrives at the station, as the charging event is not predicted over the prediction horizon, the cost function only has the first term in (6) to minimize the BTM energy consumption during the driving stage. After vehicle arrives at the station and starts charging, the same optimization problem in (6) is solved by MPC. The only difference between Case II and Case III is the maximum battery cooling power. Fig. 5 presents the state and input trajectories of these three cases, and the charging time and BTM energy consumption results are compared in Fig. 6.
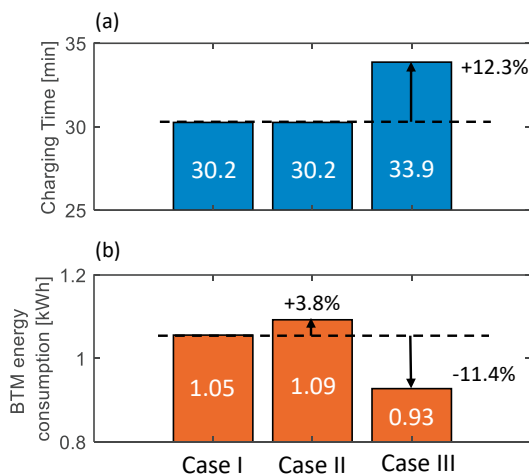

Fig. 6. Simulations results of Cases I, II, and III: (a) charging time, (b) BTM energy consumption.

It can be seen in Fig. 5 that pre-cooling is only performed in Case I, while the battery temperature in Cases II and Case III follows the upper bound constraint before arriving

at the charging station to minimize the cooling loads. While the initial battery temperatures at the beginning of the charging stage are different, Cases I and II have similar charging times. This is because the battery charging power of these two cases is almost the same, as shown in Fig. 5-(e). Compared to Case I which has a lower initial battery temperature at the start of the charging stage, Case II needs to increase the battery cooling power to avoid constraint violation, when applying the same charging power. It can be seen from Fig. 5-(d) that the battery cooling power for Case I is always below 3 kW, while the cooling power for Case II is above 4 kW during the charging stage, leading to a slight increase in the BTM energy consumption, as shown in Fig. 6-(b).

As a result, when the maximum cooling power is reduced to 3 kW in Case III, the same charging power is unattainable without pre-cooling, and the charging time is increased by 12.3%. Note that because the upper bound constraint of cooling power in Case I is inactive, the optimal performance would remain the same when the maximum cooling power is reduced from 5 kW to 3 kW. This case study illustrates that pre-cooling can distribute the cooling load over time such that the cooling demand remains within the available capacity.

4.3 Robustness of the MPC-based iPTM algorithm against selected uncertainties

In Sections 4.1 and 4.2, the effectiveness of the proposed MPC-based iPTM framework was demonstrated. While the controller successfully enforces the power and thermal constraints during the battery charging process and keeps the charging time to the desired range, such favorable performance requires preview information, e.g., vehicle speed prediction, availability of charging, etc. The previous simulations assume that accurate preview information is available. This assumption is relaxed in this subsection and the robustness of the algorithm is studied.

We consider a scenario in which the vehicle needs to wait in a queue after arriving at the station and before starting to charge. While it is assumed that the queuing time can be estimated using connectivity information, this estimate is still subject to uncertainty. The proposed scenario is illustrated in Fig. 7-(a). The total time that vehicle allowed to spend in the charging station is 40 min, including the waiting time and charging time. It is assumed that the estimated waiting time before the vehicle arrives at the station is 5 min, but the actual waiting time is 10 min. We also assume that the actual waiting time becomes available when the vehicle arrives at the charging station.

The proposed MPC-based iPTM combined with the adaptive strategy for α weight adjustment is now applied for this scenario. Simulation results are presented in Fig. 7. Note that for comparison, a reference case with fixed α is also presented in Fig. 7. In this case, α is determined assuming that the waiting time is 5 min, and will not be updated during the whole process.

Before the vehicle arrives at the station, with the estimated waiting time of 5 min, the scheduled charging time for both cases is 35 min to ensure the total time vehicle remains at the station is 40 min. However, when the vehicle arrives at the station, knowing the actual waiting time, the responses of two cases diverge. With the adaptation strategy, the controller is capable of re-scheduling the charging time to 30 min, while with a fixed α, the total time that vehicle remains at the charging station exceeds 40 min due to the uncertainty of the waiting time.
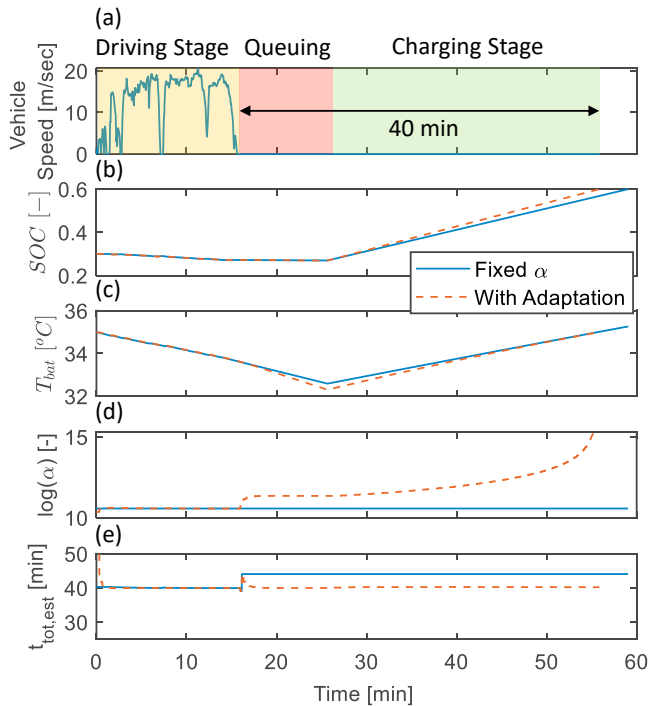
Fig. 7. State and input trajectories with different adaptive rate: (a) vehicle speed, (b) SOC, (c) battery temperature, (d) weight on charging time, and (e) estimated total time staying at charging station.

It can be seen in Fig. 7-(d) that, with adaptation strategy, α immediately rises once the controller knows the actual waiting time is longer, which forces the controller to penalize more for the charging time. Note that the values of $t_{chg,req}$ in (8) are 35 and 30 min, respectively, before and after the vehicle's arrival. This case study illustrates that the adaptive weight scheduling strategy has the ability to handle the uncertainty of waiting time for the MPC-based iPTM framework.

5. CONCLUSIONS AND FUTURE WORK

In this paper, a multi-objective model predictive control (MPC) strategy was proposed to minimize charging time and energy consumption for battery thermal management of a commercial electric vehicle (EV). The proposed method achieves a target battery state-of-charge (SOC) within the required time while enforcing the power, and thermal constraints of the battery system. The simulation results showed that the proposed MPC-based strategy, by leveraging the preview information, reduces the charging time via pre-cooling the battery before the start of the charging event. Moreover, an adaptive strategy was proposed for adjusting the weight on the charging time in the MPC stage cost to manage the trade-off between charging time and battery thermal management (BTM) energy consumption. The case study with uncertainty in the waiting time at the charging station indicated that the adaptive strategy enhances the robustness of the algorithm while meeting the operational requirements.

ACKNOWLEDGEMENTS

REFERENCES

Amini, M.R., Kolmanovsky, I., and Sun, J. (2020). Hierarchical mpc for robust eco-cooling of connected and automated vehicles and its application to electric vehicle battery thermal management. *IEEE Transactions on Control Systems Technology*, 29(1), 316–328.

Chen, C., Wei, Z., and Knoll, A.C. (2021). Charging optimization for li-ion battery in electric vehicles: a review. *IEEE Transactions on Transportation Electrification*.

Choi, H., Shin, J., and Woo, J. (2018). Effect of electricity generation mix on battery electric vehicle adoption and its environmental impact. *Energy Policy*, 121, 13–24.

Dahmane, Y., Chenouard, R., Ghanes, M., and Alvarado-Ruiz, M. (2021). Optimized time step for electric vehicle charging optimization considering cost and temperature. *Sustainable Energy, Grids and Networks*, 26, 100468.

Hamednia, A., Murgovski, N., Fredriksson, J., Forsman, J., Pourabdollah, M., and Larsson, V. (2022). Optimal thermal management, charging, and eco-driving of battery electric vehicles. *arXiv preprint arXiv:2205.01560*.

He, H., Xiong, R., and Fan, J. (2011). Evaluation of lithium-ion battery equivalent circuit models for state of charge estimation by an experimental approach. *energies*, 4(4), 582–598.

Hoke, A., Brissette, A., Smith, K., Pratt, A., and Maksimovic, D. (2014). Accounting for lithium-ion battery degradation in electric vehicle charging optimization. *IEEE Journal of Emerging and Selected Topics in Power Electronics*, 2(3), 691–700.

Keyser, M., Pesaran, A., Li, Q., Santhanagopalan, S., Smith, K., Wood, E., Ahmed, S., Bloom, I., Dufek, E., and Shirk, M. (2017). Enabling fast charging–battery thermal considerations. *Journal of Power Sources*, 367, 228–236.

Kim, J., Oh, J., and Lee, H. (2019). Review on battery thermal management system for electric vehicles. *Applied thermal engineering*, 149, 192–212.

Lee, M., Lee, H., and Won, H. (2012). Characteristic evaluation on the cooling performance of an electrical air conditioning system using r744 for a fuel cell electric vehicle. *Energies*, 5(5), 1371–1383.

Lee, Y. and Park, S. (2013). Rapid charging strategy in the constant voltage mode for a high power li-ion battery. In *2013 IEEE Energy Conversion Congress and Exposition*, 4725–4731. IEEE.

Masoudi, Y., Mozaffari, A., and Azad, N.L. (2015). Battery thermal management of electric vehicles: An optimal control approach. In *ASME Dynamic Systems and Control Conference*, volume 57243, V001T13A003.

Notter, D.A., Gauch, M., Widmer, R., Wager, P., Stamp, A., Zah, R., and Althaus, H. (2010). Contribution of li-ion batteries to the environmental impact of electric vehicles.

Parchomiuk, M., Moradewicz, A., and Gawiński, H. (2019). An overview of electric vehicles fast charging infrastructure. *2019 Progress in Applied Electrical Engineering (PAEE)*, 1–5.

Park, S. and Ahn, C. (2021). Model predictive control with stochastically approximated cost-to-go for battery cooling system of electric vehicles. *IEEE Transactions on Vehicular Technology*, 70(5), 4312–4323.

Pesaran, A.A. (2013). *Tools for designing thermal management of batteries in electric drive vehicles*. National Renewable Energy Laboratory.

Shafiei, M. and Ghasemi-Marzbali, A. (2022). Fast-charging station for electric vehicles, challenges and issues: A comprehensive review. *Journal of Energy Storage*, 49, 104136.

Tomaszewska, A., Chu, Z., Feng, X., O'kane, S., Liu, X., Chen, J., Ji, C., Endler, E., Li, R., and Liu, L. (2019). Lithium-ion battery fast charging: A review. *ETransportation*, 1, 100011.